

Quantification of Degradation and Surface Morphology of NB7 Silk Fibers Irradiated by 8 MeV Electron Beam Using XRD and SEM Techniques

Sangappa*, S. Asha, R. Somashekar¹, and Ganesh Sanjeev²

Department of Studies in Physics, Mangalore University, Mangalagangothri 574 199, India

¹Department of Studies in Physics, University of Mysore, Manasagangothri, Mysore 570 006, India

²Microtron Centre, Mangalore University, Mangalagangothri 574 199, India

(Received March 22, 2011; Revised August 29, 2011; Accepted September 4, 2011)

Abstract: NB7 silk fiber (*Bombyx mori*) was irradiated with the maximum dose range of 100 kGy using 8 MeV electron beam at room temperature. Irradiation effect in these fibers is quantified in terms of the changes in microstructural parameters employing X-ray diffraction line profile analysis technique. For this purpose we have used three asymmetric distribution functions for column lengths in a crystal. The decreasing trend of crystallite size values ($\langle N \rangle$ as well as D_s) and crystallinity with increasing dosage of radiation clearly indicates the degradation of fiber. Of the several factors responsible for such a behavior, we presume that the chain scission of polymer network is a significant one over others and it is well pronounced here, leading to low molecular weight of the samples. This degradation is attributed to many changes in tensile properties of the polymer. Comparison of SEM photographs also confirms the X-ray results.

Keywords: Fiber, Irradiation, Crystallinity, Microstructural parameters, WAXS, Degradation

Introduction

Among the natural fibers, silk has a profound place in industrial applications. Silk has excellent intrinsic properties utilizable in biotechnological and biomedical fields as well as the importance of silkworm in the manufacture of textiles [1]. There are several attempts to produce man-made fibers which have the quality and features of silk fibers by several investigators. It is well known that certain specific silk varieties have been produced which have a high yield but with less industrial applications. In this context, there is a continued interest in the field of characterization of silk to understand the properties in terms of its structural features and find ways of improving the quality of silk fibers by treatment. This 'treatment' can be of various techniques like blending with other known polymers, annealing, electro spinning, and genetic modification and also by preparing composites. Further, in recent days, there is a spurt of activities involving the exposure of silk fibers to high energetic beams. Such a study carried out by us on silk C108 belonging to bivoltine race of the *Bombyx mori* family indicated significant changes in the microcrystalline parameters [2]. Sangappa *et al.* [3-5] have reported microstructural parameters in Hosa Mysore (HM), Pure Mysore Silk (PMS), Nistari and C-nichi silk fibers. Takeshita *et al.* [6] have studied the effect of electron beam irradiation on silk fibers. Effects of gamma irradiation on biodegradation of *Bombyx mori* silk fibers have been carried out by Kojthung's group [7]. With enormous use of polymers for many purposes, recycling is challenging. Natural fibers are easy to recycle and environmental friendly. Tensile properties like tensile strain (%), elongation (mm), density etc of polymers/fibers

undergo changes when subjected to ionizing radiation. In present study attempt is made to focus on such changes in NB7 silk fiber using X-ray diffraction technique, tensile testing and scanning electron microscopy (SEM).

Experimental

Materials

NB7 silk fiber is a bivoltine class belongs to *Bombyx mori* family on the basis of shape, color, denier and life cycle of the fibers/cocoons. Cocoons were collected from the germplasm stock of the Department of Sericulture, University of Mysore, India, which were then cooked in boiling water (100 °C) for 2 min to soften the sericin and transferred to water bath at 65 °C for 2 min. Then the cocoons were reeled in warm water with the help of mono cocoon reeling equipment EPPROUVITE. These fibers were mounted on rectangular frame in just taut condition which does not involve any mechanical stretching of fibers. The whole process, starting from reeling to mounting of fibers, does not involve any type of mechanical deformation.

Electron Irradiation

Irradiation of samples was carried out at Microtron Center; Mangalore University using lanthanum hexafluoride source. The monochromatic beam is made to fall on samples kept at a particular distance with the beam features given in Table 1.

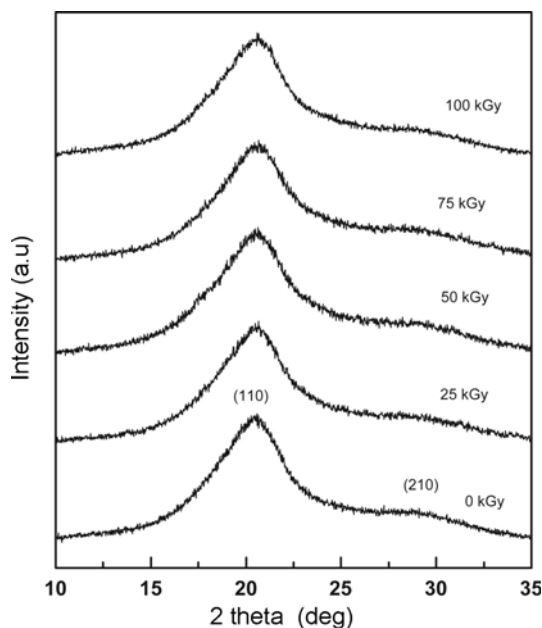
X-ray Diffraction Measurements

The XRD diffractograms of the fiber samples were recorded using Rigaku Miniflex-II X-ray diffractometer with Ni filtered, CuK α radiation of wavelength $\lambda=1.5406 \text{ \AA}$, with a graphite monochromator. The scattered beam was

*Corresponding author: syhalabhavi@yahoo.co.in

Table 1. Specifications of the electron beam accelerator and irradiation conditions

1.	Beam energy	8 MeV
2.	Beam current	20 mA
3.	Pulse repetition rate	50 Hz
4.	Pulse width	2.2 μ s
5.	Distance source to sample	30 cm
6.	Time of exposure	45 min.
7.	Dose range	0-100 kGy
8.	Atmosphere	Air
9.	Temperature	24 °C


Figure 1. XRD scans of pure and 8 MeV electron irradiated polymer samples.

focused on a detector. The samples were scanned in the 2θ range $10\text{--}50^\circ$ with a scanning speed and step size of $1^\circ/\text{min}$ and 0.02° respectively and scans are given in Figure 1.

Tensile Test

The tensile properties of pure and 8 MeV electron irradiated NB7 silk fibers were measured using INSTRON (5500R) Tensile Testing Machine. The samples were tested 5 times and mean load (gf) was taken for the interpretation of results. The specifications are temperature 27°C , humidity 65 %, single filament of length 25 mm and GL 50 mm/min.

Scanning Electron Microscopy

The morphology of the pure and 8 MeV electron irradiated *Bombyx mori* silk fiber was observed with a scanning electron microscope (SEM, JSM-6390LV) at 15 kV. All the samples were sputtered with gold.

Theory

Microstructural parameters such as crystal size ($\langle N \rangle$) and lattice strain (g in %) are usually determined by employing Fourier method of Warren and Averbach [8,9], and Warren [10]. The intensity of a profile in the direction joining the origin to the center of the reflection can be expanded in terms of Fourier cosine series;

$$I(s) = \sum_{n=-\infty}^{\infty} A(n) \cos\{2\pi n d(s-s_0)\} \quad (1)$$

where the coefficients of the harmonics $A(n)$ are functions of the size of the crystallite and the disorder of the lattice. Here, s is $\sin(\theta)/(\lambda)$, s_0 being the value of s at the peak of a profile; n is the harmonic order of co-efficient and d is the lattice spacing. The Fourier coefficients can be expressed as;

$$A(n) = A_s(n) \cdot A_d(n) \quad (2)$$

For a Paracrystalline material, $A_d(n)$ can be obtained, with Gaussian strain distribution [11],

$$A_d(n) = \exp(-2\pi^2 m^2 n g^2) \quad (3)$$

Here, m is the order of the reflection and $g = (\Delta d/d)$ is the lattice strain. Normally one also defines mean square strain $\langle \varepsilon^2 \rangle$, which is given by g^2/n . This mean square strain is dependent on n , whereas not g [12,13]. For a probability distribution of column lengths $P(i)$, we have;

$$A_s(n) = 1 - \frac{nd}{D} - \frac{d}{D} \left[\int_0^n i P(n) di - n \int_0^n P(i) di \right] \quad (4)$$

where $D = \langle N \rangle d_{hkl}$ is the crystallite size and i is the number of unit cells in a column. In the presence of two orders of reflections from the same set of Bragg planes, Warren and Averbach [8,9] have shown a method of obtaining the crystal size ($\langle N \rangle$) and lattice strain (g in %). But in polymer it is very rare to find multiple reflections. So, to determine the finer details of microstructure, we approximate the size profile by simple analytical function for $P(i)$ by considering only the asymmetric functions. Another advantage of this method is that the distribution function differs along different directions. Whereas, a single size distribution function that is used for the whole pattern fitting, which we feel, may be inadequate to describe polymer diffraction patterns [12-14]. Here it is emphasized that the Fourier method of profile analysis (single order method used here) is quite reliable one as per the recent survey and results of Round Robin test conducted by IUCr [15]. In fact, for refinement, we have also considered the effect of background by introducing a parameter (see for details regarding the effect of background on the microcrystalline parameters [16]). For the sake of completeness, we reproduce the following equations which are used in the computation of micro structural parameters.

The Exponential Distribution

It is assumed that there are no columns containing fewer than p unit cells and those with more decay exponentially. Thus, we have [17],

$$P(i) = \begin{cases} 0 & ; \text{if } i < p \\ \alpha \exp\{-\alpha(i-p)\} & ; \text{if } i \geq p \end{cases} \quad (5)$$

where, $a = 1/(N-p)$ Substituting this in equation (4), we get;

$$A_s(n) = \begin{cases} A(0)(1-n/\langle N \rangle) & ; \text{if } n \leq p \\ A(0)\{\exp[-\alpha(n-p)]\}/(\alpha N) & ; \text{if } n \geq p \end{cases} \quad (6)$$

Here, α is the width of the distribution function, i is the number of unit cells in a column, n is the harmonic number, p is the smallest number of unit cells in a column and $\langle N \rangle$, the number of unit cells counted in a direction perpendicular to the (hkl) Bragg plane.

The Lognormal Distribution

The Lognormal distribution function is given by;

$$P(i) = \frac{1}{(2\pi)^{1/2} \sigma^i} \exp\left\{-\frac{[\log(i/m)]^2}{2\sigma^2}\right\} \quad (7)$$

where, σ is the variance and m is the median of the distribution function.

Substituting for $P(i)$ in equation (4) and simplifying [5], we get,

$$A_s(n) = \frac{m^3 \exp[(9/4)(2^{1/2} \sigma)^2]}{3} \operatorname{erfc}\left[\frac{\log(|n|/m)}{2^{1/2} \sigma} - \frac{3}{2} 2^{1/2} \sigma\right] - \frac{m^2 \exp(2^{1/2} \sigma)^2}{2} |n| \operatorname{erfc}\left[\frac{\log(|n|/m)}{2^{1/2} \sigma} - 2^{1/2} \sigma\right] + \frac{|n|^3}{6} \operatorname{erfc}\left[\frac{\log(|n|/m)}{2^{1/2} \sigma}\right] \quad (8)$$

The above equation is the one used by Ribarik *et al.* [12] The maximal value $A_s(0)$ is given by;

$$A_s(0) = \frac{2m^3 \exp[(9/4)(2^{1/2} \sigma)^2]}{3} \quad (9)$$

The area-weighted number of unit cells in a column is given by

$$\langle N \rangle_{surf} = \frac{2m \exp[(5/4)(2^{1/2} \sigma)^2]}{3} \quad (10)$$

and the volume-weighted number of unit cell in a column is given by

$$\langle N \rangle_{vol} = \frac{3m \exp[(7/4)(2^{1/2} \sigma)^2]}{4} \quad (11)$$

The Reinhold Distribution

With the exponential distribution function, $P(i)$ rises

discontinuously at p , from zero to its maximum value. In contrast, the Reinhold function allows a continuous change by putting,

$$P(i) = \begin{cases} 0 & ; \text{if } i \leq p \\ \beta^2(i-p) \exp\{-\beta(i-p)\} & ; \text{if } i > p \end{cases} \quad (12)$$

where $\beta = 2/N - p$ substituting these in equation (4), we obtain

$$A_s(n) = \begin{cases} A(0)(1-n/\langle N \rangle) & ; \text{if } n \leq p \\ [A(0)(n-p+2/\beta)/N] \{\exp[-\beta(n-p)]\} & ; \text{if } n \geq p \end{cases} \quad (13)$$

where, β is the width of the distribution which has been varied to fit the experimental results. p is the smallest number of unit cells in a column, $\langle N \rangle$ is the number of unit cells counted in a direction perpendicular to the (hkl) Bragg plane; d is the spacing of the (hkl) planes; λ is the wavelength of X-rays used; i is the number of unit cells in a column; n is the harmonic number and D_s is the surface weighted crystal size ($\langle N \rangle d_{hkl}$).

All the distribution functions were put to test in order to find out the most suitable crystal size distribution function for the profile analysis of the X-ray diffraction. The procedure adopted for the computation of the parameters is as follows. Initial values of g and N were obtained using the method of Nandi *et al.* [18]. With these values in the equations give numbers earlier give the corresponding values for the width of distribution. These are only rough estimates, so the refinement procedure must be sufficiently robust to start with such values. Here we compute;

$$\Delta^2 = [I_{cal} - (I_{exp} + BG)]^2 / npt \quad (14)$$

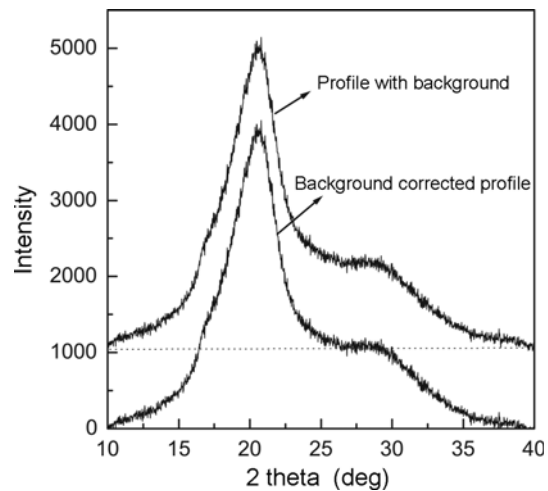


Figure 2. Profile with background and background corrected NB7 silk fiber.

Table 2. Microstructural parameters of pure and electron irradiated polymer samples by various distribution functions

Sample	Exponential						Reinhold				Lognormal			
	2θ	d_{hkl}	$\langle N \rangle$	g in %	D_s (Å)	delta	$\langle N \rangle$	g in %	D_s (Å)	delta	$\langle N \rangle$	g in %	D_s (Å)	delta
0 kGy	20.42	4.346	11.04±0.99	1.0±0.10	47.98	0.09	11.24±1.01	2.0±0.18	48.84	0.09	11.58±2.08	3.0±0.54	50.32	0.18
25 kGy	20.66	4.296	6.74±0.61	2.0±0.18	28.96	0.09	7.21±0.72	4.0±0.40	30.97	0.10	6.55±0.77	3.0±0.36	28.14	0.12
50 kGy	20.64	4.299	6.06±0.42	2.0±0.14	26.05	0.07	6.21±0.49	3.0±0.24	26.69	0.08	6.04±0.66	4.0±0.44	25.97	0.11
75 kGy	20.68	4.291	6.19±0.49	3.0±0.24	26.56	0.08	6.40±0.58	4.0±0.36	27.55	0.09	6.08±0.67	4.0±0.44	26.08	0.11
100 kGy	20.58	4.310	6.01±0.42	3.0±0.21	25.90	0.07	6.22±0.43	4.0±0.28	26.81	0.07	5.68±0.45	3.0±0.24	24.48	0.08

where, BG represents the error in the background estimation (Figure 2), n_{pt} is number of data points in a profile, I_{cal} is intensity calculated using equations (1)-(13) and I_{exp} is the experimental intensity. The values of were divided by half the maximum value of intensity so that it is expressed relative to the mean value of intensities, and then minimized.

X-ray Profile Analysis

For the analysis, we have used X-ray diffraction data in the above equations to simulate the intensity profile by varying the necessary parameters till one gets a good fit with the experimental profile. For this purpose, a multidimensional algorithm SIMPLEX is used for minimization [19]. We have used pure and 8 MeV electron beam irradiated NB7 silk fiber samples. The computed crystal imperfection parameters along with reported physical parameters are given in the Table 2 for different distribution functions for each of the samples.

Results and Discussion

X-ray Profile Analysis Study

Figures 3(a)-(d), 4(a)-(d) and 5(a)-(d) show the simulated and experimental profiles for 8 MeV electron irradiated and pure polymer samples fitted using different asymmetric analytical distribution functions. The simulated profile was obtained with the equations given in Ref. [5] using appropriate model parameters. This procedure was followed for all other samples treated at different radiation doses. The computed microcrystalline parameters such as crystallite size $\langle N \rangle$ (number of unit cells), lattice strain g in %, the width of the crystallite size distribution (α) and the standard deviation are given in Table 2. It is evident from Table 2 that all the asymmetric distributions used, give more or less similar results. By and large, Exponential distribution function gives a better fit than Reinhold/Lognormal distributions. Here we would like to emphasize that the standard deviation in all the cases for the microstructural parameters are given

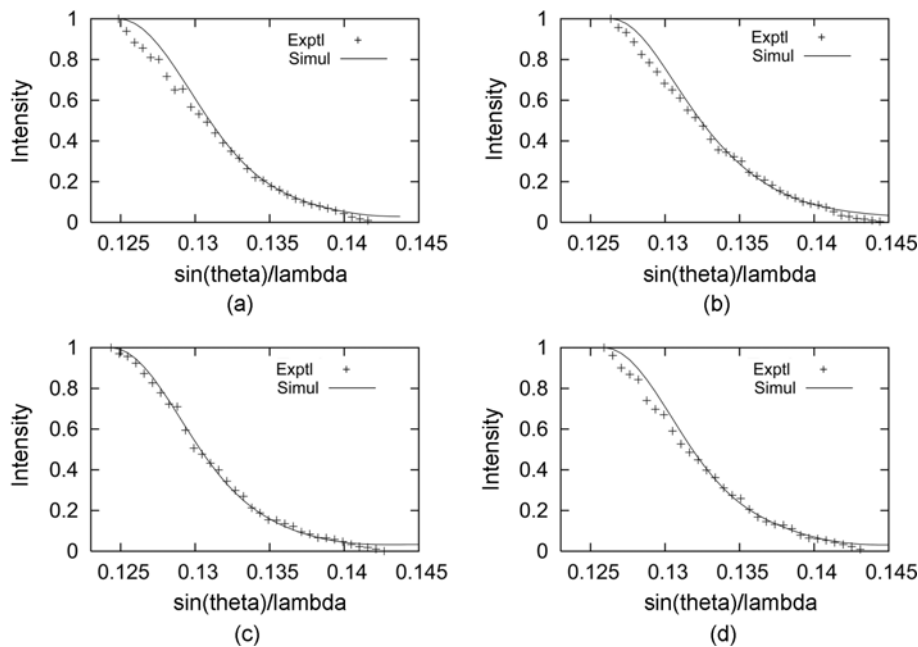


Figure 3. (a)-(d) Experimental and simulated intensity profiles of X-ray reflection of Silk fiber samples obtained with exponential column length distribution function.

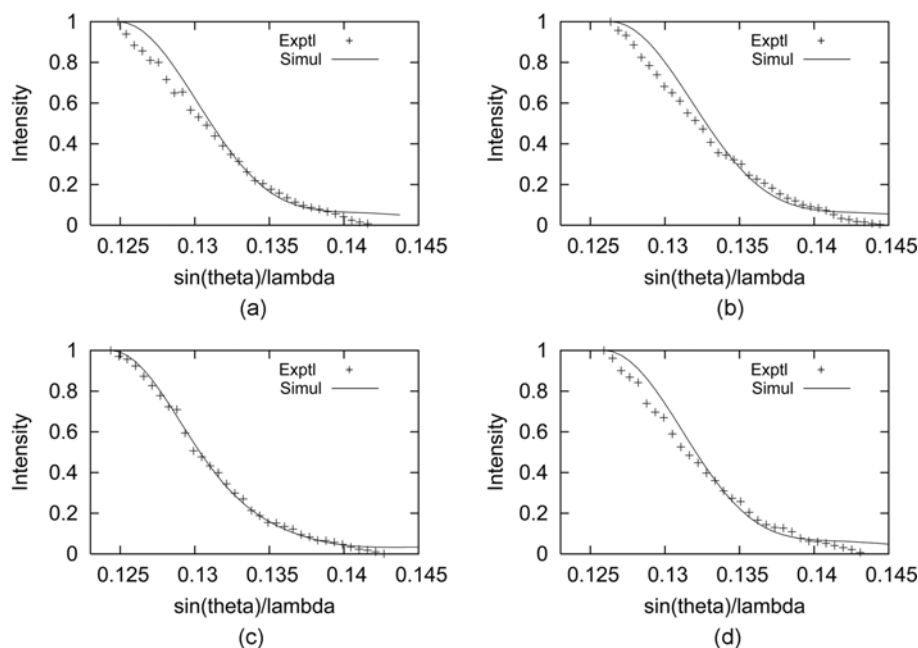


Figure 4. (a)-(d) Experimental and simulated intensity profiles of X-ray reflection of silk fiber samples obtained with reinhold column length distribution function.

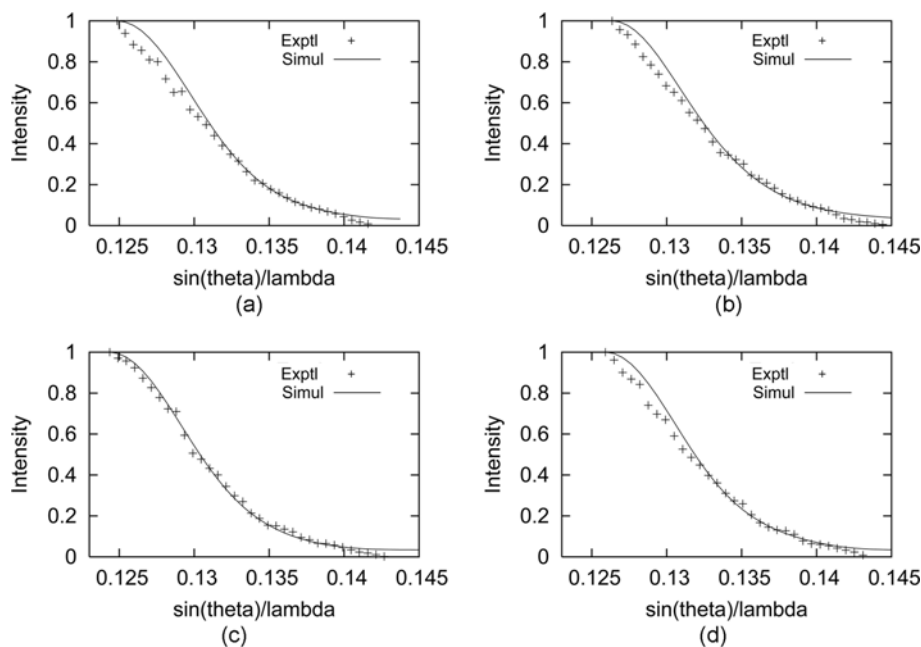


Figure 5. (a)-(d) Experimental and simulated intensity profiles of X-ray reflection of Silk fiber samples obtained with Lognormal column length distribution function.

in Table 2 as delta. Since Exponential distribution function gives a better fit than others, we used the corresponding results given in Table 2 to infer some important conclusions. From the Table 2, two important features are to be noted. They are

- (i) The value of the surface weighted crystallite size D_s (Å) decreases as irradiation dose increases,

- (ii) The value of the crystallite size $\langle N \rangle$ is more for unirradiated polymers

Irradiation of polymers mainly causes two important changes. (1) Degradation of the polymer, wherein main chain scission takes place, leading to low molecular weight polymer. (2) Cross-linking, which is chemical bonding between polymeric chains to form network polymers. Both

of these effects cause changes in physical properties. Degradation of polymer leads to loss in mechanical strength, whereas cross linking improves the physical properties. Quite often these effects may occur simultaneously. The final result depends on the nature of the material, on the amount radiation, dosage rate and energy of the radiation. From the Table 2 it is evident that the crystallite size decreases as irradiation dose increases. Normally the strength of the fibers, irrespective of natural or man-made, increases with increase in crystallite size [20]. This suggests that the unirradiated fiber has higher tenacity than irradiated fibers.

The variation of lattice strain (ϵ) lies between 1.0-4.0 % in the case of Exponential distribution for polymer samples. From the Table 2, it is clear that the lattice strain and its variation for various values of the radiation doses (kGy) in polymer samples are very small.

The X-ray diffraction patterns in Figure 1 show crystalline peaks, superimposed on an amorphous halo. The crystallinity of NB7 *Bombyx mori* silk fiber with and without irradiation was studied with wide angle X-ray scattering (WAXS) measurements. An estimation of the degree of crystallinity (X_c) was recorded from the ratios of the areas under the crystalline peak and the respective halos using the method [21]

$$X_c = \frac{A_c}{A_c + A_a} \times 100 \quad (15)$$

where A_c and A_a are the area of crystalline and amorphous (halo) regions respectively. From the Table 3 the crystallinity decreases with dose rate. In the virgin sample the crystallinity is 72 % and it reaches to 59 % at a 100 kGy dose. This is due to the degradation and breaking (fracture) of polymer network started due to electron irradiation.

Tensile Properties

Tensile properties, particularly tensile strength and elongation are the most important for evaluating the performance of fibers for proper applications. Table 4 illustrates the extension (mm) and tensile strain (%) of both untreated and electron irradiated silk fibers. From the Table 4 it is evident that the tensile properties of the fibers change as irradiation dose increases. For the pure sample extension is 3.4 mm and tensile strain is 13.6 %. In case of electron irradiated sample

Table 3. Most intense peaks and crystallinity of pure and 8 MeV electron irradiated NB7 silk fibers

Sample	2θ	d in Å	Crystallinity (%)
0 kGy	20.42	4.345	72.00
25 kGy	20.65	4.298	66.00
50 kGy	20.50	4.328	64.00
75 kGy	20.71	4.284	62.00
100 kGy	20.64	4.290	59.00

Table 4. Tensile properties of pure and 8 MeV electron irradiated NB7 silk fibers

Sample	Extension (mm)	Tensile strain (%)
0 kGy	3.40	13.60
25 kGy	3.05	12.20
50 kGy	2.89	11.60
75 kGy	2.90	9.20
100 kGy	2.67	10.71

(50 kGy) extension is 3.05 mm and tensile strain is 12.2 % and in the case of 100 kGy irradiated sample extension is 2.67 mm and tensile strain is 10.71 %. The changes in tensile properties are due to breaking of weak hydrogen bonds [22]. Ionizing radiation such as gamma radiation directly affects the decreasing tensile strength of the fibroin fibers. This was due to weakness of peptide bonding in fibroins polypeptides, reduction of β -sheet structure in the silk fibroin, as well as the release of low-molecular weight proteins in degradation products. The results of this study show that degradation of fibroin increases with increasing radiation doses [7]. Our results clearly states that changes observed are due to degradation of the fiber sample.

Scanning Electron Microscopic Analysis

We have studied the changes in the surface morphology of the *Bombyx mori* NB7 silk fibers before and after 8 MeV electron beam irradiation by scanning electron microscopy (SEM). Figure 6(a) shows the surface morphology of a virgin mulberry silk fiber. The fiber surface is smooth and no fracture was observed. Figure 6(b), (c), (d) shows the surface structure of mulberry silk fibers irradiated with electron beam. A comparison of 6(a) and 6(b), (c), (d) immediately reveals that the fiber structure morphology of the silk fibers was strongly affected by the electron irradiation. When the

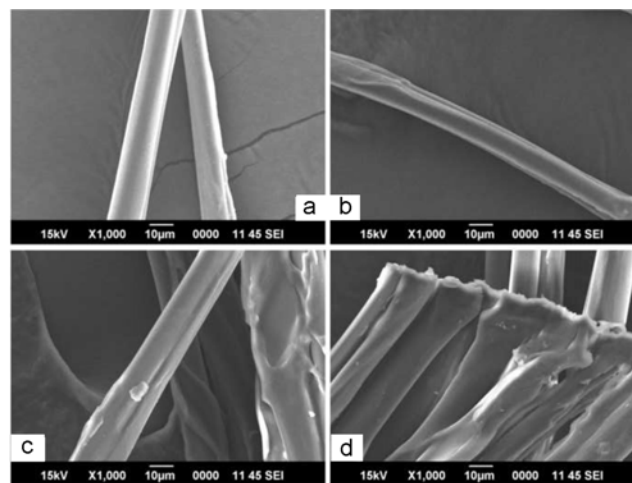


Figure 6. SEM micrographs of pure and electron irradiated samples.

electron dose was as low as (25 kGy) there were only small fractures on the silk fiber surface. When the irradiation dose was as high as 100 kGy, the fibers exhibited a deeper fractures and no smooth surface. From these observations, we can conclude that the electron irradiation has affected the surface morphology of the fibers.

Conclusion

The main intension of this study is to investigate the influences of the electron irradiation on the structural and mechanical properties of NB7 silk fibers. From the wide angle X-ray scattering (WAXS) study of electron irradiated silk fiber (*Bombyx mori*) samples, we have observed that even though there is not much change in the position of the X-ray reflections, a decreasing trend in the value of crystallinity and microstructural parameters occurs. The significant change in crystallinity and microstructural parameters in polymer is due to the effect of electron irradiation. This causes the degradation of small polymer units leading to the formation of low polymer network. It is found that among the three different asymmetric distribution functions, Exponential gives a better fit in these polymer samples. It can be observed that electron irradiation treatment have significant effect on the tensile properties. The tensile test clearly indicates that tensile property of the fibers changes as irradiation dose increases.

From the SEM analysis it is clear that electron irradiated fiber surface shows fractures and it is much pronounced as irradiation dose increases indicating that there are both surface as well microscopic degradation of NB7 silk fiber. Essentially, the treatment and the results tend to a situation wherein the applicability of the method in textile industries is not so encouraging in this particular situation.

Acknowledgements

The authors are thankful to University Grant Commission, New Delhi, Govt of India, for providing financial assistance through a project F. No. 33-14/2007 (SR). Also authors wish to thank Head and technical staff, Microtron Center, Mangalore University for the electron irradiation of samples.

References

1. D. Lance Miller, S. Putthanarat, and W. W. Adoms, *Bio*

2. Sangappa, S. Asha, Ganesh Sanjeev, G. Subramanya, P. Parameswara, and R. Somashekar, *J. Appl. Polym. Sci.*, **115**, 2183 (2010).
3. Sangappa, K. Okuyama, and R. Somashekar, *J. Appl. Polym. Sci.*, **91**, 3045 (2004).
4. Sangappa, S. S. Mahesh, and R. Somashekar, *J. Bioscience* **30**, 259 (2005).
5. Sangappa, S. S. Mahesh, R. Somashekar, and G. Subramanya, *J. Polym. Res.*, **12**, 465 (2005).
6. H. Takeshita, K. Ishida, Y. Kamiishi, F. Yoshii, and T. Kume, *Macromolecular Materials and Eng.*, **283**, 126 (2000).
7. A. Kojthung, P. Meesilpa, B. Sudatis, L. Treeratanapiboon, R. Udomsangpetch, and B. Oonkhanond, *Int. J. Biodeterioration and Biodegradation*, **62**, 487 (2008).
8. B. E. Warren and B. L. Averbach, *J. Appl. Phys.*, **21**, 595 (1950).
9. B. E. Warren, *Acta Cryst.*, **8**, 483 (1955).
10. B. E. Warren, Addison-Wesley New York, 1969.
11. I. H. Hall and R. Somashekar, *J. Appl. Cryst.*, **124**, 1051 (1991).
12. R. Ribarik, T. Ungar, and J. Gubicza, *J. Appl Cryst.*, **34**, 669 (2001).
13. N. C. Popa and D. Balzar, *J. Appl Cryst.*, **35**, 338 (1995).
14. P. Scardi and M. Leoni, *Acta Crystallogr Sect A*, **57**, 604 (2001).
15. D. Balzar, *IUCr News Lett.*, **228**, 14 (2002).
16. R. Somashekar, I. H. Hall, and P. D. Carr, *J. Appl. Cryst.*, **22**, 363 (1989).
17. R. Somashekar and H. Somashekarappa, *J. Appl. Crystallogr.*, **130**, 147 (1997).
18. R. K. Nandi, H. K. Kho, W. Schlosberg, G. Wissler, J. B. Cohen, and B. Jr Crist, *J. Appl. Cryst.*, **17**, 22 (1984).
19. W. Press, B. P. Flannery, S. Teukolsky, and W. T. Vetterling, Eds., "Numerical Recipes", Cmbridge University Press, 1986.
20. K. G. Lee, R. Jr Barton, and J. M. Schultz, *J. Poly. Sci. (B)*, **33**, 1 (1995).
21. P. H. Hermans and A. Weidinger, *Makromol. Chem.*, **24**, 44 (1961).
22. C. Yumusak and V. Alekberow, *Fiber. Polym.*, **9**, 15 (2008).